

Supplemental methods

Protein production and characterization

A11 cMb was engineered by using site-directed mutagenesis to add a cysteine residue (GGGGSGGC) to the C-terminus of the parental anti-PSCA A11 minibody [1]. The vector pSecTag2 A (Thermo Fisher) was used to transfect human embryonic kidney 293-F cells (Life Technologies). Stably transfected 293-F cells were cultured in serum-free media. The collected supernatant was loaded onto a HiTrap Protein L column (GE Healthcare) in phosphate buffered saline (PBS) using an ÄKTA Purifier (GE Healthcare). A11 cMb protein was eluted with 0.1 M Glycine, pH 2.0, neutralized in 1 M Tris, pH 8.2, and dialyzed three times against PBS.

Dynamic light scattering of A11 cMb (7.5 nm) was accomplished on a particle size analyzer (Brookhaven ZetaPALS) and compared with Bovine Serum Albumin (66 kDa, 6.2 nm) and another minibody fragment (GA101Mb ~80 kDa, 7.2 nm), and size distribution by number was analyzed on BIC Particle Sizing Software (**Figure S1D**).

Mass spectrometry of A11 cMb and A11 cMb-Cy5.5 was completed at City of Hope. Samples were reduced and alkylated using iodoacetamide, then digested using trypsin and GluC. Unmodified cysteines in the protein were reduced and alkylated prior to analysis, resulting in a mass shift of +57. Modified cysteines, such as the C-terminal cysteine in A11 cMb-Cy5.5, show a mass shift of +1038 from the mal-Cy5.5 conjugation.

Cell lines and tumor models

Male nu/nu mice (*Foxn1^{nu}*, Jackson Laboratories) were used for all tumor models. The 22Rv1 human prostate cell line (ATCC) was previously transduced with retrovirus to express PSCA (22Rv1-PSCA) [2]. To establish tumors, $0.5-1 \times 10^6$ 22Rv1 or 22Rv1-PSCA cells in 1:1 PBS:Matrigel (BD Bioscience) were implanted s.c. in the shoulder of 8- to 10-week-old male

nu/nu mice (25-30 g) and allowed to grow for 3-4 weeks. Mice were fed alfalfa-free food to reduce autofluorescence in the stomach contents, although they still emitted fluorescent signal.

22Rv1-PSCA was transfected with Firefly Luciferase (FLuc)-IRES-GFP (22Rv1-PSCA-FLuc) as previously described [3]. For the orthotopic intraprostatic model, 5×10^3 22Rv1-PSCA-FLuc cells in 5 μ l Hank's Buffered Saline Solution (Sigma) were surgically implanted into the anterior lobe of the prostate [4]. Mice were monitored weekly by bioluminescence, and tumors were allowed to grow for 6 weeks post-implantation.

The PC3 human prostate cell line (ATCC) was previously transfected to express PSCA [2] and FLuc to produce the PC3-PSCA-FLuc cell line. $0.5-1 \times 10^6$ PC3 and PC3-PSCA-FLuc cells in 1:1 PBS:Matrigel were implanted in the shoulder of male nu/nu mice and allowed to grow for 3-4 weeks.

Quantitation of PSCA cell surface expression

22Rv1-PSCA antigen binding capacity (ABC) (Quantum Simply Cellular, Bangs Laboratories), representative of the PSCA cell surface density, was quantified by flow cytometry as $2.1 \times 10^6 \pm 2.5 \times 10^5$ (n=2) similar to previous published results [1]. PC3-PSCA-FLuc was quantified to have an ABC of $5.2 \times 10^5 \pm 2.6 \times 10^5$ (n=3).

Histology and IHC

Freshly isolated tumors and organs of interest were fixed in 10% formalin/PBS. Samples were embedded in paraffin (UCLA Translational Pathology Core Laboratory) and sectioned into 4 μ m sections, which were then stained with H&E or anti-PSCA antibody (ab56338, Abcam).

Supplemental references

1. Knowles SM, Zettlitz KA, Tavare R, Rochefort MM, Salazar FB, Stout DB, et al. Quantitative immunoPET of prostate cancer xenografts with ⁸⁹Zr- and ¹²⁴I-labeled anti-PSCA A11 minibody. *J Nucl Med.* 2014; 55: 452-9.
2. Saffran DC, Raitano AB, Hubert RS, Witte ON, Reiter RE, Jakobovits A. Anti-PSCA mAbs inhibit tumor growth and metastasis formation and prolong the survival of mice bearing human prostate cancer xenografts. *Proceedings of the National Academy of Sciences of the United States of America.* 2001; 98: 2658-63.
3. Knowles SM, Tavare R, Zettlitz KA, Rochefort MM, Salazar FB, Jiang ZK, et al. Applications of immunoPET: using ¹²⁴I-anti-PSCA A11 minibody for imaging disease progression and response to therapy in mouse xenograft models of prostate cancer. *Clin Cancer Res.* 2014; 20: 6367-78.
4. Park SI, Kim SJ, McCauley LK, Gallick GE. Pre-clinical mouse models of human prostate cancer and their utility in drug discovery. *Curr Protoc Pharmacol.* 2010; Chapter 14: Unit 14 5.

Supplemental figures

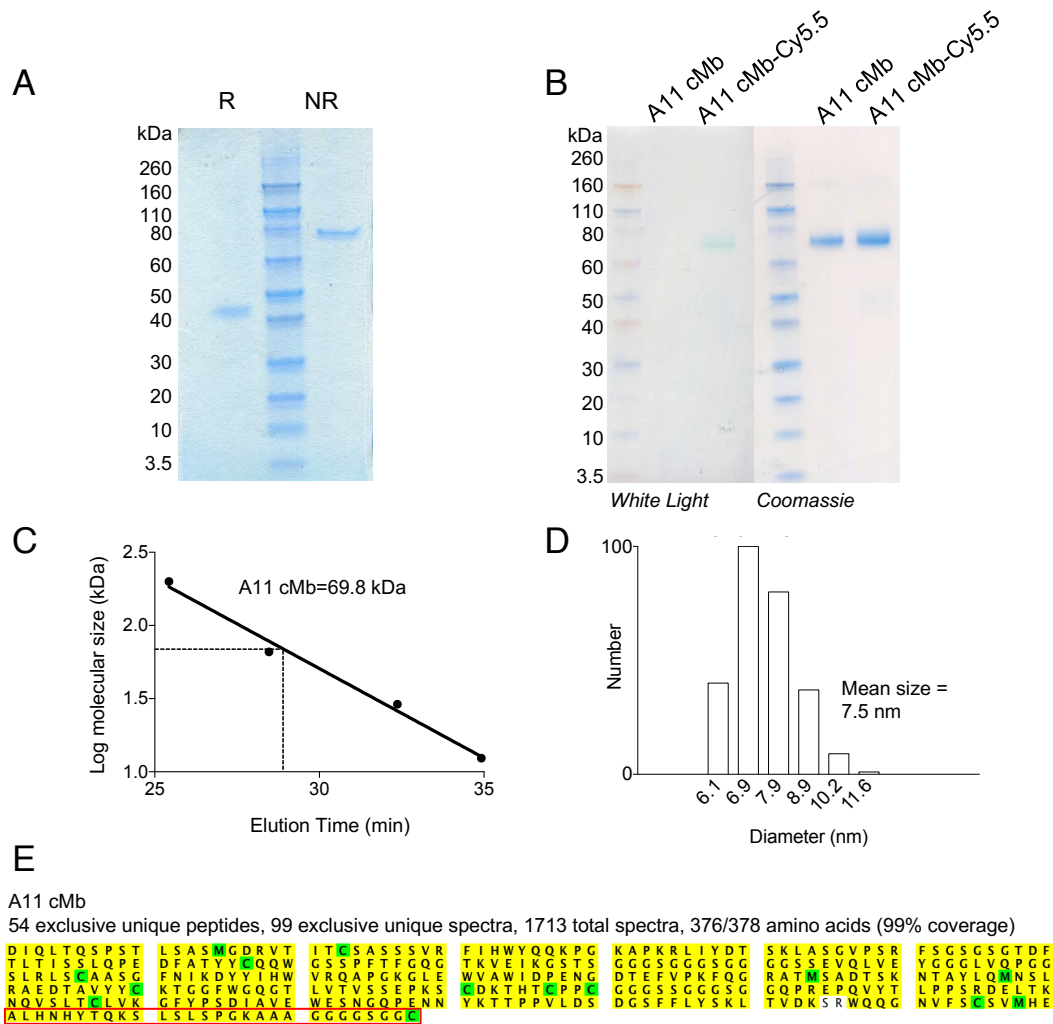


Figure S1. Protein characterization of A11 cMb. (A) Purity and correctly assembly of A11 cMb was confirmed by SDS-PAGE. Under non-reducing conditions (NR), A11 cMb migrated as a covalently bound scFv-C_H3 homodimer approximately at 80.02 kDa, the molecular weight calculated from the sequence. Under reducing conditions (R), A11 cMb migrated as a scFv-C_H3 monomer. (B) The Cy5.5 label seen by unstained (white light) SDS-PAGE corresponds to the A11 cMb-Cy5.5 protein band visualized by Coomassie. (C) The size of A11 cMb was estimated to be 70 kDa from interpolation with the SEC standards of 200, 66, and 29 kDa. (D) The mean hydrodynamic diameter of A11 cMb was estimated to be 7.5 nm as measured by dynamic light scattering, with a size distribution ranging from 6.1-11.6 nanometers (nm). (E) Mass spectrometry of peptides resulting from trypsin and GluC digests covered all cysteine residues (highlighted green in the displayed A11 cMb sequence; covered residues highlighted in yellow). Only the peptide (boxed in red) with the C-terminal cysteine showed a mass shift of +1038, which was observed in the A11 cMb-Cy5.5 sample and not the A11 cMb sample.

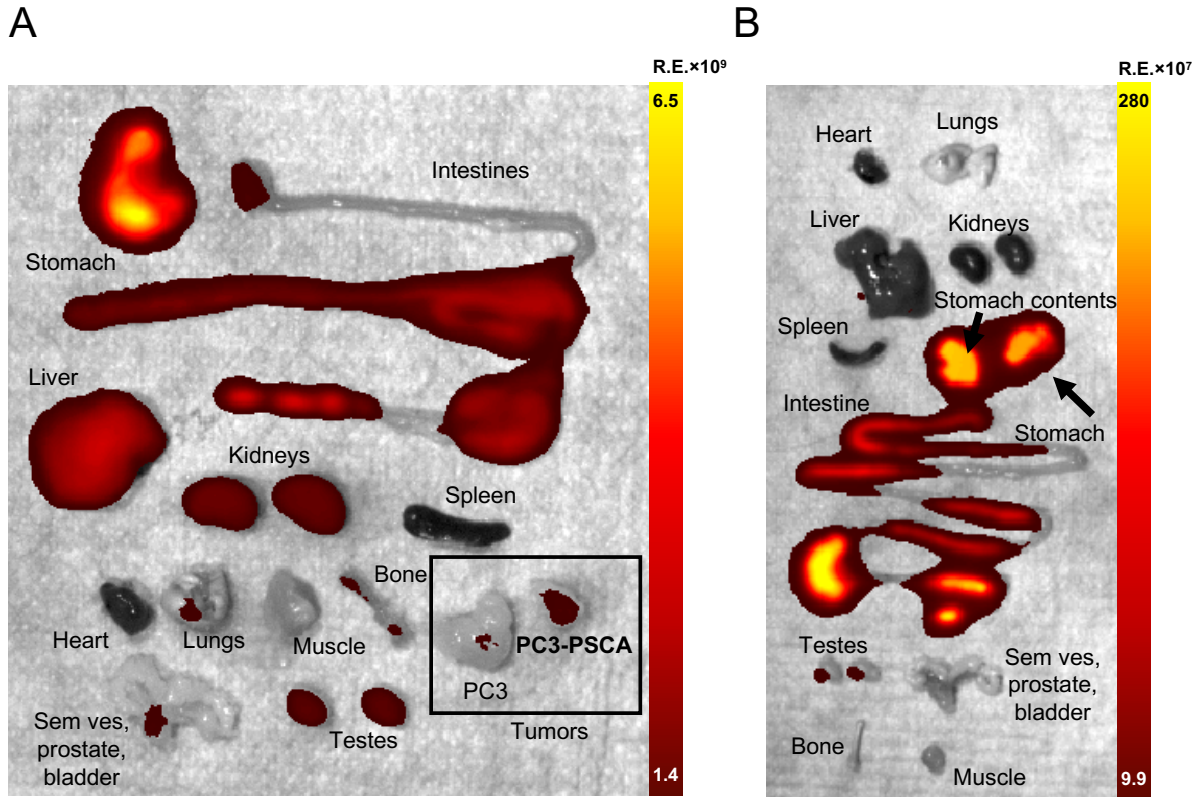


Figure S2. Fluorescence ex vivo biodistribution of ^{124}I -A11 cMb-Cy5.5 compared with autofluorescence. (A) Resected organs from a representative PC3-PSCA tumor-bearing mouse (Figure 4) were imaged by Cy5.5 fluorescence. Fluorescent signal is specific to the PC3-PSCA tumors, compared with low signal in PC3 control tumors and background tissues. Fluorescent signal is also present in the organs of clearance: liver, kidney, and bladder. High autofluorescence is present in the stomach and intestines due to the food, despite the use of alfalfa-free pellets. (B) For comparison, a non-tumor-bearing mouse without probe injection was imaged using the same Cy5.5 fluorescent settings, confirming autofluorescence in the stomach, intestine, and testes. Scale units R.E.: Radiance Efficiency ($\frac{\text{photons/sec/cm}^2/\text{sr}}{\mu\text{w/cm}^2}$).

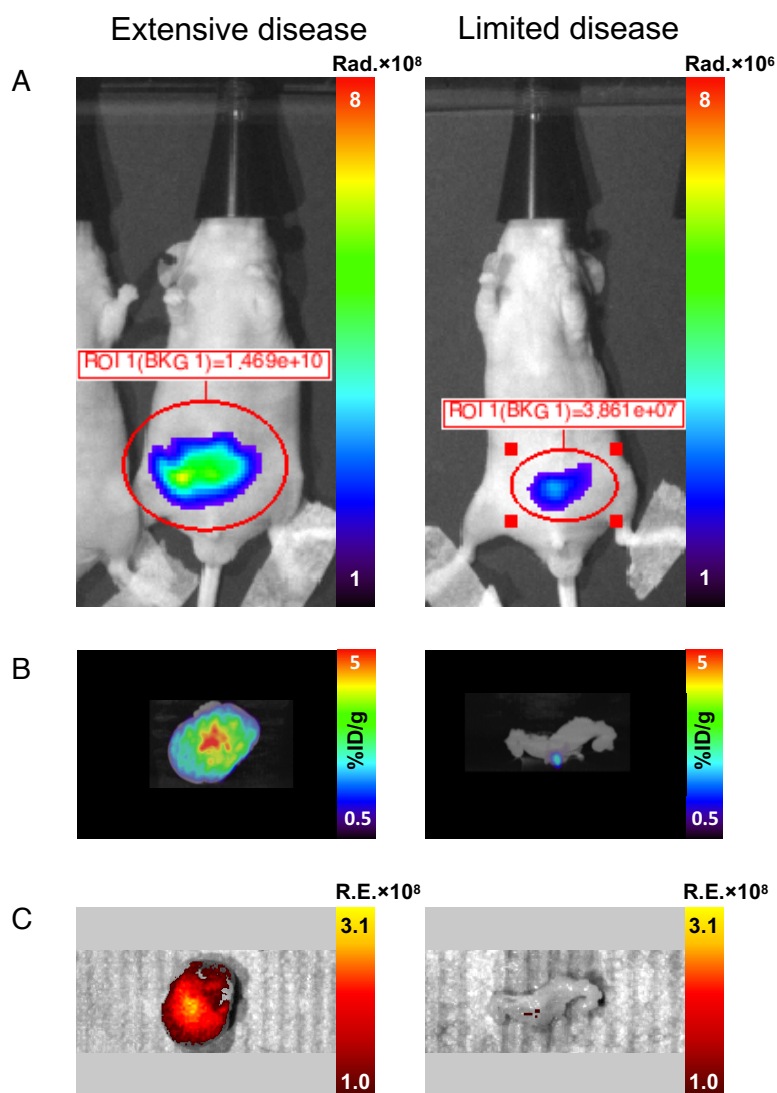


Figure S3: Comparison of orthotopically implanted intraprostatic tumors. (A) 22Rv1-PSCA-GFP-Fluc intraprostatic tumors were imaged weekly by bioluminescence to determine the time point for PET/fluorescence imaging. A representative prostate tumor in a mouse (Figure 5) with extensive disease was quantified in comparison to the bioluminescent signal from a tumor with limited disease, resulting in a 2 log difference of radiance signal. Scale units Rad= radiance. (B, C) The bioluminescence signal from extensive disease correlates with the corresponding ^{89}Zr -A11 cMb-Cy5.5 PET and fluorescence images of the resected prostate tumor. Scale units Rad.: Radiance (photons/sec/cm²/sr); R.E.: Radiance Efficiency ($\frac{\text{photons/sec/cm}^2/\text{sr}}{\mu\text{w/cm}^2}$).